Journal of Nano- and Electronic Physics
Vol. **4** No 4, 04027(8pp) (2012)

Журнал нано- та електронної фізики
Том **4** № 4, 04027(8cc) (2012)

Simulation of Ferrofluids in Confined Domains

T.V. Lyutyy*, V.V. Reva, A.Yu. Polyakov

Sumy State University, 2, Rimsky-Korsakov Str., 40007 Sumy, Ukraine

(Received 10 December 2012; in final form 26 December 2012; published online 29 December 2012)

The equilibrium properties of ferromagnetic fluids are investigated using the method of molecular dynamics and techniques for parallel computing with graphics processing units. In particular, the magnetization curve and the magnetic susceptibility of such medium are studied. The influence of the vessel's shape, external fields applied in orthogonal directions, volume fraction of particles, and properties of the surfactant coating, which provides repulsion, are discussed. It is shown that properties of the system are determined by the nature of particles clustering arising from the dipole interaction. It is established that the internal parameters of a liquid carrier, thermal and dimensional effects determine the equilibrium properties of ferrofluid through the effects on its internal structure.

Keywords: Ferromagnetic fluid, Susceptibility, Molecular dynamic simulation, CUDA, Barnes-Hut algorithm.

PACS numbers: 47.65.Cb, 83.10.Mj, 75.50.Tt

1. INTRODUCTION

Dispersed structures, which represent the ensemble of ferromagnetic nanoparticles suspended in a liquid, are called ferromagnetic fluids or ferrofluids [1]. Such systems combine simultaneously properties of a liquid (viscosity, fluidity, surface tension) and properties of a ferromagnetic (internal magnetic field, large magnetic permeability, controllability by external magnetic fields). Therefore, ferromagnetic liquids are sufficiently attractive mediums from the point of view of various practical applications, whose spectrum extends from the rocket fuel supply in the zero-gravity conditions to the macromolecule separation [2], new therapy methods, such as the targeted drug delivery [3] and magnetic fluid hyperthermia [4].

Description of the properties of ferrofluids as uniform continuous mediums is well developed within the ferrohydrodynamics theory proposed in [1]. However, the stated approximation ignores possible collective effects conditioned by the interaction of particles in a liquid, does not give the possibility to investigate structural properties of ferrofluid and character of possible particle clusterization. The given effects are very important for confined volumes of ferrofluid. A number of models which take into account the interaction are known in literatures. Their common feature is the use of the known theory of the Weiss paramagnetic gas [5]. In the following, either multiplication of the argument of the Langevin function by the phenomenological multiplier responsible for the interaction was carried out [6] or modifications of the method of a mean dipole field were applied [7, 8]. Results obtained by using the mentioned approximations qualitatively coincide with the experimental ones for sufficiently diluted ferrofluids, but, however, they do not allow to obtain the information concerning their structure.

Complexities of the analytical description stimulate the development of numerical methods. The well-known Monte Carlo method [9] is widely used for the description of the equilibrium properties of ferromagnetic liquids. On the basis of the simplicity of its software implementation and comparatively low requirements to the computational capability, the vast majority of the numerical experiments starting from the 80s [10, 11] up to now [12] was carried out with the use of this method. At the same time, the Monte Carlo method does not allow to consider non-equilibrium processes and, moreover, technical problems of description of the cluster behavior in ferromagnetic liquids arise [13].

Another well-known method of numerical simulation, namely, the method of molecular dynamics [9], is free of the mentioned disadvantages, but, however, it is more resource-intensive. Therefore, its wide application for the investigation of the properties of ferromagnetic liquids began about 10 years ago. As a rule, two its variants are used: the Brownian dynamics method [14] and the Langevin simulation [15]. In the present work, we use exactly the last technique, since it has simpler physical interpretation.

The aim of the present work is the description of the equilibrium and structural properties of ferromagnetic liquids confined into an elongated vessel by using the molecular dynamics method and solving the Langevin equations for each particle of the ensemble. The work has the following structure. In Section 2 we present the physical justification of the model, basic equations, and dimensionless equations suitable for a direct numerical simulation. In Section 3 we describe the features of the realization methods of high-performance computations in the modeling of sufficiently large volumes of ferrofluids. Section 4 contains the results and their analysis, in particular, influence of different factors on the magnetic susceptibility of ferrofluid is descripted. In the Section 5 we present the conclusions which follow from the performed investigations.

2. DESCRIPTION OF THE MODEL

Based on the hypothesis that a liquid carrier is stationary or for the description of the equilibrium properties of ferrofluids, it is enough to specify the equations

* lyutyy@oeph.sumdu.edu.ua

of motion and equations of the magnetic moment dynamics for each ferromagnetic particle from N particles, which generate an ensemble, suspended in a liquid with viscosity η. As a rule, in the real situation all particles are produced of the same material and, in the first approximation, they can be considered to be uniform with density D and magnetization μ.

We will consider some (i-th) particle of the volume V_i, mass $M_i = V_iD$, inertia moment $I_i = \iiint_{V_i} dVDr_1^2$ (r_1 is the distance of a particle element dV to the rotation axis), and magnetic moment $\mathbf{m}_i = V_i\mu$. Let in the chosen Cartesian coordinate system position of the particle center is specified by the radius-vector $\mathbf{r}_i$. The particle will be in the total dipole field generated by the magnetic moments of other particles. Taking into account the external field $\mathbf{H}^{ext}$, the resulting field acting on the magnetic moment of the chosen particle takes the form

$$\mathbf{H}_i = \sum_{j=1, j\neq i}^{N} \frac{3\mathbf{r}_j(\mathbf{m}_j\mathbf{r}_{ij}) - \mathbf{m}_j r_{ij}^2}{r_{ij}^5} + \mathbf{H}^{ext}, \qquad (1)$$

where $\boldsymbol{r}_{ij} = \boldsymbol{r}_i - \boldsymbol{r}_j$ is the radius-vector connecting the centers of the i-th and j-th particles. The force which is conditioned by the field of the form (1) will be determined as [1]

$$\mathbf{F}_i^{dip} = -\mu_0(\mathbf{m}_i\nabla)\cdot\mathbf{H}_i, \qquad (2)$$

where $\mu_0 = 4\pi\cdot10^{-7}$ H/m is the magnetic constant and $\nabla = \mathbf{e}_x\partial/\partial x + \mathbf{e}_y\partial/\partial y + \mathbf{e}_z\partial/\partial z$ is the nabla operator. After implementation of the corresponding differentiation procedures, expression (2) can be re-written in the form of

$$\mathbf{F}_i^{dip} = \sum_{j=1, j\neq i}^{N}\left[3\frac{\mathbf{r}_{ij}(\mathbf{m}_j\mathbf{m}_i) + \mathbf{m}_i(\mathbf{m}_j\mathbf{r}_{ij}) + \mathbf{m}_j(\mathbf{m}_i\mathbf{r}_{ij})}{r_{ij}^5} - 15\frac{\mathbf{r}_{ij}(\mathbf{u}_j\mathbf{r}_{ij})(\mathbf{u}_i\mathbf{r}_{ij})}{r_{ij}^7}\right]. \qquad (3)$$

Exactly the long-range dipole force (3) conditions the behavior of ferrofluids with a sufficiently large volume fraction of particles.

To prevent the undesirable agglomeration of particles of the ensemble under the action of the dipole force (3), particles are covered by special non-magnetic shell which provides repulsion. As a rule, such repulsion has a rapidly decreasing behavior and is modeled using the Lenard-Jones potential [5]. Explicit form of the resulting repulsive force is the following [15]:

$$\mathbf{F}_i^{sr} = 24e\sum_{j=1, j\neq i}^{N}\frac{\mathbf{r}_{ij}}{r_{ij}^2}\left[\left(\frac{s}{r_{ij}}\right)^{12} - \left(\frac{s}{r_{ij}}\right)^{6}\right]. \qquad (4)$$

Here e is the potential well depth; s is the distance between particle centers at which $\mathbf{F}_i^{sr} = 0$.

The gravity and buoyancy forces with the prevalence of the first one also act on the particle in the vertical direction. However, since sedimentation of ferromagnetic particles is not observed in real ferrofluids [16], one can neglect the resulting action of two stated forces.

The resistance force of liquid to the motion of translation for small particle velocities is taken to be proportional to the first time derivative of the radius-vector with the proportionality coefficient G_i^t which depends on the liquid properties and particle shape.

Finally, it is convenient to represent the interaction with thermostat by the action of random force $\mathbf{X}_i^t$ with statistical characteristics [17]

$$\langle X_{i\alpha}^t\rangle = 0,$$
$$\langle X_{i\alpha}^t(t)X_{i\beta}^t(t)\rangle = 2k_BTG_i^t\delta_{\alpha\beta}\delta(t-t), (\alpha,\beta = x,y,z). \qquad (5)$$

Here $\delta(\,)$ is the Dirac delta-function; $\delta_{\alpha\beta}$ is the Kronecker delta-symbol; $k_B = 1{,}38\cdot10^{-23}$ J/K is the Boltzmann constant; T is the thermodynamic temperature.

Taking into account the aforesaid, equation which describes the motion of translation of the chosen particle will have the following form:

$$M_i\frac{d^2\mathbf{r}_i}{dt^2} = \mathbf{F}_i^{dip} + \mathbf{F}_i^{sr} - G_i^t\frac{d\mathbf{r}_i}{dt} + \mathbf{X}_i^t. \qquad (6)$$

Rotatory motion of each particle in this case obeys the system of equations [3] relative to the azimuth (φ_i) and polar (θ_i) angles

$$I_i\frac{d^2\varphi_i}{dt^2} = N_{iz} - G_i^r\frac{d\varphi_i}{dt} + \mathbf{X}_i^r, \qquad (7)$$

$$I_i\frac{d^2\theta_i}{dt^2} = -N_{ix}\sin\varphi_i + N_{iy}\cos\varphi_i - G_i^r\frac{d\theta_i}{dt} + \mathbf{X}_i^r, \qquad (8)$$

where $\mathbf{N}_i$ is the mechanical moment which acts on the particle and whose components, respectively, are equal to $N_{ix} = m_{iy}H_{iz} - m_{iz}H_{iy}$, $N_{iy} = m_{iz}H_{ix} - m_{ix}H_{iz}$, and $N_{iz} = m_{ix}H_{iy} - m_{iy}H_{ix}$ ($m_{x,y,z}$ are the projections of the vector of magnetic moment on the axes of the Cartesian coordinate system); G_i^r is the coefficient of liquid resistance to the rotatory motion; $\mathbf{X}_i^r$ is the random force moment which models the interaction of the i-th particle with the thermostat $\mathbf{X}_i^t$ with statistical characteristics [15]

$$\langle X_{i\alpha}^t\rangle = 0,$$
$$\langle X_{i\alpha}^t(t)X_{i\beta}^t(t)\rangle = 3k_BTG_i^r\delta_{\alpha\beta}\delta(t-t), (\alpha,\beta = \theta,\varphi). \qquad (9)$$

Here, difference in the numerical coefficient of the noise intensity in comparison with expression (5) is connected with the presence of only two angular coordinates instead of three translational, while thermal energy should be shared in equal ratio between rotatory motion and motion of translation.

Dynamics of the magnetization of each particle obeys the Landau-Lifshitz equation [18]

$$\frac{d\mathbf{m}_i}{dt} = -\gamma\mathbf{m}_i\times(\mathbf{H}_i^{\text{eff}} + \mathbf{X}_i^m) - \frac{\lambda\gamma}{m_i}\mathbf{m}_i\times(\mathbf{m}_i\times\mathbf{H}_i^{\text{eff}}), \qquad (10)$$

where $\gamma = 1{,}76\cdot10^{11}$ rad T^{-1} s^{-1} is the gyromagnetic ratio; λ (> 0) is the dimensionless damping parameter; $\mathbf{H}_i^{\text{eff}} = \partial W_i/\partial\mathbf{m}_i$ is the effective magnetic field acting on the magnetic moment; W_i is the particle magnetic energy; $\mathbf{X}_i^m$ is the random magnetic field which represents the thermostat action.

To simplify the subsequent calculations and simulation, we will suggest that all particles are ball-shaped of the same radius R, and, as a result, the same magnitude of the magnetic moment $m_i = m = 4\pi R^3\mu/3$, the same mass $M_i = M = \frac{4}{3}\pi R^3 D$, inertia moment $I_i = I = \frac{2}{5}mR^2 = \frac{2}{5}\cdot\frac{4}{3}\pi R^3 DR^2 = \frac{8}{15}\pi R^5 D$, coefficient of liquid resistance to the motion of translation, according to the Stokes law, $G_i^t = G^t = 6\pi\eta R$, and, finally, the same coefficient of liquid resistance to the rotatory motion $G_i^r = G^r = 8\pi\eta R^3$.

For the convenience of the consequent analysis, it is reasonable to write equations (6)-(10) in dimensionless form with taking into account the following substitutions: $\boldsymbol{\rho}_i = \mathbf{r}_i/R$; $\mathbf{u}_i = \mathbf{m}_i/m$; $\tau = t/T_{ch}$,

$$T_{ch} = R/\mu(3D/4\mu_0)^{0,5} \tag{11}$$

is the characteristic period of the mechanical motion; $\Gamma = 2\pi\eta RT_{ch}/DV$ is the reduced coefficient of resistance (here $V = 4\pi R^3/3$ is the particle volume); $\mathbf{h}_i = 3\mathbf{H}_i/4\pi\mu$; $\mathbf{h}^{ext} = 3\mathbf{H}^{ext}/4\pi\mu$; $\sigma = s/R$; $\varepsilon = eT_{ch}^2/VDR$; $\mathbf{h}_i^{\text{eff}} = 3\mathbf{H}_i^{\text{eff}}/4\pi\mu$; $\boldsymbol{\Xi}_i^m = 3\mathbf{X}_i^m/4\pi\mu$; $\tau_1 = t/T_{ch1}$,

$$T_{ch1} = 3/(4\pi\mu\gamma) \tag{12}$$

is the characteristic period of the magnetic moment precession. As a result, equations describing dynamics of the chosen particle take the form

$$\frac{d^2\boldsymbol{\rho}_i}{d\tau^2} = \mathbf{f}_i^{dip} + \mathbf{f}_i^{sr} - 3\Gamma\frac{d\boldsymbol{\rho}_i}{d\tau} + \frac{T_{ch}^2}{VRD}\boldsymbol{\Xi}^t, \tag{13}$$

where

$$\mathbf{f}_i^{dip} = \sum_{j=1,j\neq i}^{N}\left[3\frac{\boldsymbol{\rho}_{ij}(\mathbf{u}_j\mathbf{u}_i) + \mathbf{u}_i(\mathbf{u}_j\boldsymbol{\rho}_{ij}) + \mathbf{u}_j(\mathbf{u}_i\boldsymbol{\rho}_{ij})}{\rho_{ij}^5} - 15\frac{\boldsymbol{\rho}_{ij}(\mathbf{u}_j\boldsymbol{\rho}_{ij})(\mathbf{u}_i\boldsymbol{\rho}_{ij})}{\rho_{ij}^7}\right], \tag{14}$$

$$\mathbf{f}_i^{sr} = 24\varepsilon\sum_{j=1,j\neq i}^{N}\frac{\boldsymbol{\rho}_{ij}}{\rho_{ij}^2}\left[\left(\frac{\sigma}{\rho_{ij}}\right)^{12} - \left(\frac{\sigma}{\rho_{ij}}\right)^{6}\right], \tag{15}$$

$$\frac{2}{5}\frac{d^2\varphi_i}{d\tau^2} = u_{ix}h_{iy} - u_{iy}h_{ix} - 4\Gamma\frac{d\varphi_i}{d\tau} + \frac{T_{ch}^2}{VR^2D}\Xi_\varphi^r, \tag{16}$$

$$\frac{2}{5}\frac{d^2\theta_i}{d\tau^2} = -(u_{iy}h_{iz} - u_{iz}h_{iy})\sin\varphi_i + (u_{iz}h_{ix} - u_{ix}h_{iz})\cos\varphi_i - 4\Gamma\frac{d\theta_i}{d\tau} + \frac{T_{ch}^2}{VR^2D}\Xi_\theta^r, \tag{17}$$

where

$$\mathbf{h}_i = \sum_{j=1,j\neq i}^{N}\frac{3\boldsymbol{\rho}_j(\mathbf{u}_j\boldsymbol{\rho}_{ij}) - \mathbf{u}_j\rho_{ij}^2}{\rho_{ij}^5} + \mathbf{h}^{ext}, \tag{18}$$

$$\frac{d\mathbf{u}_i}{dt} = -\gamma\mathbf{u}_i\times(\mathbf{h}_i^{\text{eff}} + \boldsymbol{\Xi}_i^m) - \lambda\gamma\mathbf{u}_i\times(\mathbf{u}_i\times\mathbf{h}_i^{\text{eff}}). \tag{19}$$

Taking into account the property of the Dirac delta-function $\delta(t) = \delta(\tau T_{ch}) = \delta(\tau)/T_{ch}$, correlation functions of the random forces and force moments in equations (13), (16), and (17) are equal to, respectively,

$$\langle\Xi_\alpha^t(\tau)\Xi_\alpha^t(\tau')\rangle = 6k_B T\Gamma\delta_{\alpha\beta}\delta(\tau-\tau')/T_{ch}\ (\alpha,\beta = x,y,z), \tag{20}$$

$$\langle\Xi_\alpha^r(\tau)\Xi_\beta^r(\tau')\rangle = 12k_B T\Gamma\delta_{\alpha\beta}\delta(\tau-\tau')/T_{ch}\ (\alpha,\beta = \varphi,\theta). \tag{21}$$

Comparing characteristic times T_{ch1} and T_{ch} for real magnetic materials, one can conclude that

$$T_{ch} >> T_{ch1}.$$

For example, for maghemite (γ-Fe_2O_3) with magnetization $\mu = 3{,}1\cdot10^5$ A/m and density $D = 5\cdot10^3$ kg/m^3 at the particle size of $R = 10$ nm by using (11), we obtain that $T_{ch} = 9{,}942\cdot10^{-10}$, while with taking into account (12) $T_{ch1} = 4{,}376\cdot10^{-18}$. The given fact allows to exclude from the consideration magnetic dynamics described by the equation (19), since magnetic moment relaxes rather rapidly to its equilibrium position which is determined almost completely by magnetocrystalline anisotropy. In other words, one can consider magnetic moment inside the particle to be stationary in the time scale of the mechanical motion.

3. TECHNIQUES OF THE NUMERICAL SIMULATION

3.1 Parallel computing with graphics processor units

Simulation of ferrofluid within the above described model, in essence, is the many body problem. Systems with gravitational interaction, systems of electrons, etc. belong to this class of problems. The problem accompanying the simulation of such ensembles is the calculation time which is proportional to N^2. This fact makes almost impossible to simulate systems of many elements even using very powerful personal computers. Calculation time can be decreased by applying traditional distributed computing, for example, with the use of clusters or supercomputers. However, this solution has economic restrictions, since the pointed systems have high prices and expensive maintenance.

Use of the graphics processor units (GPU) is an alternative to this approach. GPU represent the complex of the same modules (the so-called, kernels) performed on one crystal, each of which is intended for the implementation of a limited set of mathematical operations. Initially, these devices are applied for high-speed calculations necessary for realistic object mapping in the real-time mode, and therefore, GPU are widely used in video adapters (or video cards) of personal computers. Growth of the level of detail of the images is closely connected with the growth of computations that constantly stimulates the increase in the GPU efficiency. In its turn, increase in production is provided due to the increase in the number of GPU kernels. Therefore, modern video cards contain hundreds and even thousands of kernels [19] and provide computational power which is one order of magnitude more than in special processors.

Initially, architecture of GPU is oriented on the implementation of parallel computing that is the reason of the GPU use in the problems which are not connected with mapping of graphics but require a huge amount of computations – the so-called general calculations.

Until recently, production of software, which uses the possibilities of GPU, has required special skills and

knowledge. However, after the release of the Compute Unified Device Architecture (CUDA) technique – the product of the known producer of video cards NVIDIA Company, – situation has been significantly simplified [20]. Now, it is possible to organize high-performance parallel computing with the use of the widespread programming languages, such as C/C++ or Fortran.

The aforesaid together with relative cheapness of video cards led to the situation that currently general calculations on GPU is the rapidly developing direction in the field of high-performance computing. Thus, for example, 52 of 500 the most powerful supercomputers use exactly GPU [21].

3.2 Application of the Barnes-Hut algorithm

Due to the use of approximate calculation algorithms of the pairwise particle interaction one can obtain considerable acceleration of computing. Because of the inverse proportionality of the dipole field to the third degree of the distance (see (18)), substantial correlations of the magnetic moment directions will be observed only for nanoparticles located sufficiently close to each other. At the same time, if some localized group of particles is remoted enough from the chosen one, then there is no necessity of detailed calculation of pairwise interaction of the chosen particle with each particle from the group. It is possible to substitute the action of the group of particles for the action of pseudoparticle located in the geometric center of the group and possessing magnetic moment equal to the mean over the whole group.

The given idea together with intuitively clear recursive algorithm was proposed for the first time for the evolution simulation of space objects, such as stars and galaxies, where interaction occurs due to the gravitational interaction [22], and took the name Barnes-Hut algorithm. Here separation of particles for groups takes place by the division of space into cubic cells with their further division into 8 equal cubic sub-cells until each cell, irrespective of the size, will contain no more than 1 particle. The angular size of cubic cells with respect to the position of the chosen particle from the largest to the smallest ones is checked in the calculations of the interaction of the chosen particle with others. If angular size of some particle is rather small, then we calculate interaction between the chosen particle and pseudoparticle corresponding to the whole cell. Otherwise, all 8 subcells forming the chosen cell are sequentially analyzed. Calculation time in this case increases not as N^2, but as $N \cdot \log N$ that gives a considerable advantage for ensembles of thousands and tens of thousands particles.

We note that it is possible to achieve greater acceleration of computing using the so-called fast multipole method [23]. In the framework of this technique, calculation time is proportional to N. In contrast to the described Barnes-Hut algorithm, where interaction either between particle and particle or between particle and group of particles is calculated, here interaction between groups of particles is obtained. However, in spite of the obvious advantage in time, a question about the correctness of taking into consideration the correlations of particle magnetic moments during the formation of clusters of different configurations using the fast multipole method is still open. Therefore, in the present work we have chosen just the Barnes-Hut algorithm.

The detailed description of the applications of this algorithm for parallel computing with using the CUDA technique can be found in the work [24] and in the references there. All calculations were carried out using the budgetary commercial video card NVIDIA GeForce GTS 450 which contains 192 kernels.

4. RESULTS AND DISCUSSION

The proposed model together with the described technique of parallel computing was realized in the software code on C++. Using the written program, it is possible not only to specify different external and internal parameters of the ensemble and calculate the averaged characteristics, but also analyze the dynamics of nanoparticles in liquid.

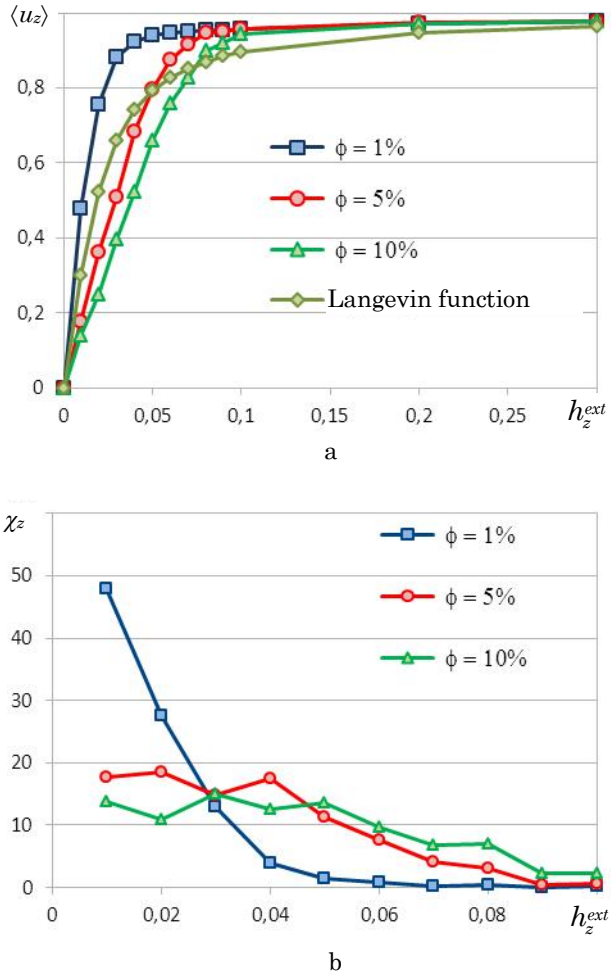

Fig. 1 – Influence of the volume fraction of nanoparticles in ferroliquid on its magnetization (a) and susceptibility (b)

Below we present the simulation results of the ensemble of $N = 10^4$ maghemite particles (γ-Fe_2O_3) with the following parameters: $\mu = 3{,}1 \cdot 10^5$ A/m, $D = 5 \cdot 10^3$ kg/m^3, $R = 5 \cdot 10^{-9}$ m, which are suspended in liquid (viscosity $\eta = 0{,}89 \cdot 10^{-3}$ Pa·s). It was considered that ensemble is located in cylindrical vessel, whose height exceeds five times the diameter, unless otherwise specified. Oz-axis of the Cartesian coordinate system is directed along the vessel height. Parameters in (15) were taken to be equal

to $\sigma = 2{,}1$, $\varepsilon = 0{,}005$, and temperature $T = 300$ K, unless otherwise specified. Equilibrium state for the specified parameters was obtained during $3 \cdot 10^4$ iterations, and the averaged characteristics were determined by the last $2 \cdot 10^4$ iterations.

Intensity of the dipole interaction depends on the average interparticle spacing, and the larger volume content of particles, the less interparticle spacing

$$\phi = \frac{4\pi R^3 N}{3V_f} \cdot 100\% , \qquad (22)$$

where V_f is the liquid volume. Under the condition that $\phi \to 0$, the average value of the reduced magnetization $\langle u_i \rangle$ along the i-th coordinate axis is described by the Langevin function [5]

$$\langle u_i \rangle = \coth \alpha - 1/\alpha , \quad \alpha = \mu_0 m H_i^{ext} / k_B T , \qquad (23)$$

where H_i^{ext} is the external field along the i-th axis.

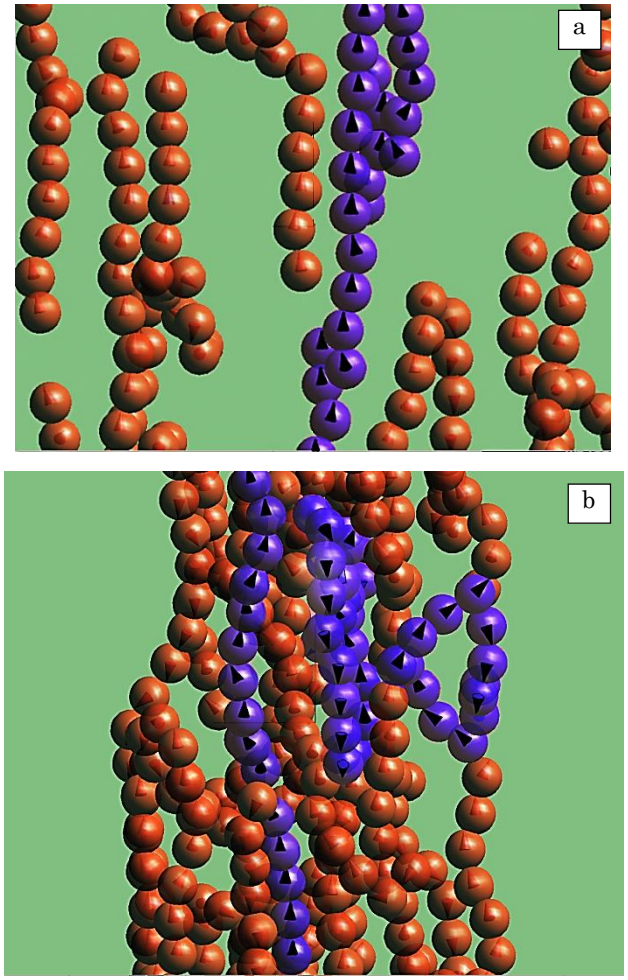

Fig. 2 – Typical structure of particles in liquid at $\phi = 1\%$ (a) and $\phi = 5\%$ (b)

In Fig. 1a we show the dependences of the reduced magnetization on the external field for different volume contents of particles. As seen from the figure, increase in the magnetization, as a rule, is the result of interaction in comparison with the case without interaction. This is connected with the fact that dipole field of particles, whose magnetic moments are mainly oriented along the external field, coincides with the latter in direction and amplifies it. As a result, in the equilibrium state for the given simulation conditions particles form linear chains (see Fig. 2a). However, with the increase in ϕ for not very large external fields, antiferromagnetic character of the dipole interaction can affect, at which the resulting direction of adjacent chains can be opposite. Moreover, large concentration of particles can condition the formation of closed ring-shaped clusters (see Fig. 2b). All this leads to the decrease in the ensemble magnetization. Therefore, with the increase in ϕ ensemble magnetization increases slower that is expressed in flatter dependence of the differential magnetic susceptibility of the ensemble

$$\chi_z = \frac{\Delta \langle u_z \rangle}{\Delta h_z^{ext}} , \qquad (24)$$

see Fig. 1b. We have to note that the described mechanism can lead to the situation that the calculated value of the reduced magnetization can be less than the predicted by expression (23).

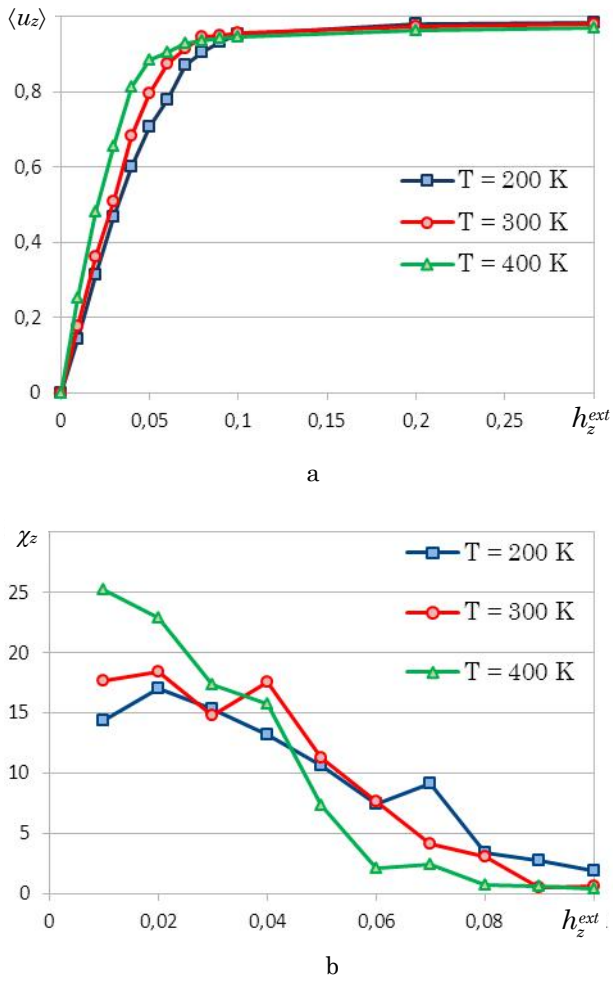

Fig. 3 – Influence of the thermostat temperature on the magnetization (a) and susceptibility (b) of ferroliquid. $\phi = 5\%$

In the case, when thermal energy does not exceed magnetostatic one conditioned by the dipole interaction, the role of thermal effects is insignificant. Quantitative

criterion which expresses this fact is the interaction-to-thermal energy ratio of two neighboring particles

$$\Lambda = \frac{\mu_0 m^2}{16\pi R^3 k_B T}. \qquad (25)$$

It is known [16] that if the condition $\Lambda << 1$ holds, then particles undergo Brownian motion, otherwise they form clusters determining the ferrofluid structure. By using expression (25) it is not difficult to show that for the stated simulation parameters in the temperature range of 200-400 K parameter Λ takes the values of 1,91-0,955. Therefore, difference in the magnetization curves for these temperatures is observed only for small values of the external field (see Fig. 3a). Since aggregation of particles into clusters is complicated with temperature increase, response to the external field becomes more expressed that leads to the susceptibility increase with temperature (see Fig. 3b). For large fields, when reduced magnetization tends to unit, thermal fluctuations tend to disorder the ensemble. This conditions insignificant decrease in the magnetization with temperature when $\langle u_z \rangle \approx 1$ (see Fig. 3a).

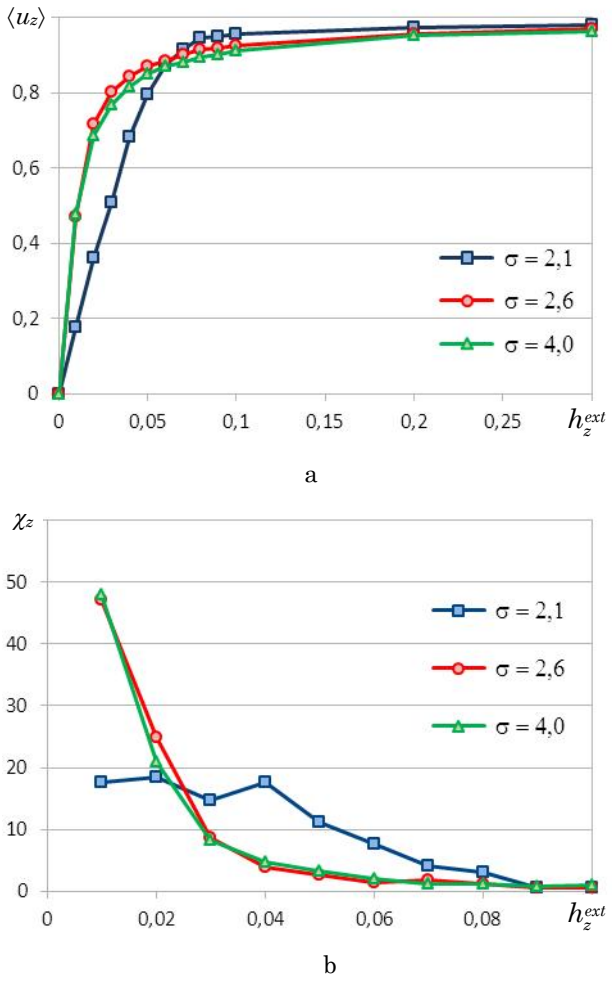

Fig. 4 – Influence of the parameter σ in the Lenard-Jones potential on the magnetization (a) and susceptibility (b) of ferrofluid. $\phi = 5\%$

The feature of the dipole interaction consists in the fact that it leads to the mutual attraction between particles. At the same time, repulsion occurs due to special coatings of particles and is modeled using the Lenard-Jones potential. Distance σ, on which attraction force is compensated by the repulsion one, is one of the main phenomenological parameters in the mentioned potential. Increase in this parameter leads to the decrease in the role of dipole interaction, since mean interparticle spacing increases and aggregation of stable clusters is complicated. As a result, this leads to the increase in the susceptibility (see Fig. 4b) as well as in the case of the temperature increase. For sufficiently large external fields, when $\langle u_z \rangle \approx 1$, dipole field amplifies the external one, and, therefore, condition $\langle u_z(\sigma_1) \rangle > \langle u_z(\sigma_2) \rangle$ holds, if $\sigma_1 < \sigma_2$ (see Fig. 4a).

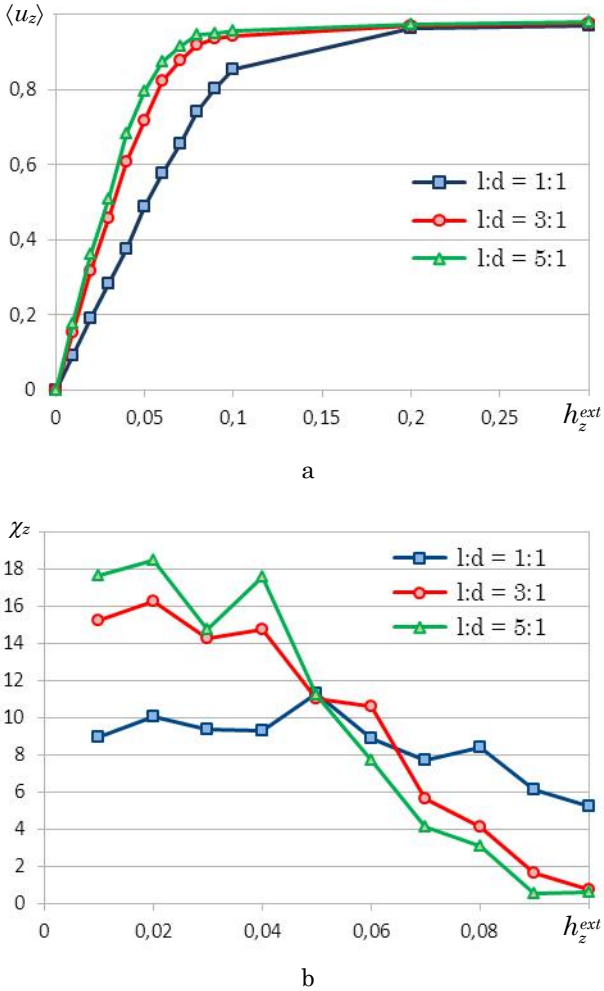

Fig. 5 – Influence of the form-factor on the magnetization (a) and susceptibility (b) of ferrofluid. $\phi = 5\%$

Due to the presence of the internal structure, ferrofluid can demonstrate the dependence of the properties on the vessel shape, and anisotropy of the properties conditioned by the form-factor as well. If, not changing the total vessel volume and number of particles, change the ratio between orthogonal linear sizes, two mutually exclusive tendencies will be observed in the system. On the one hand, increase in one linear size will promote the formation of chains along this direction. As a result, reduced magnetization (Fig. 5a) increases with the increase in the "height":"diameter" (l:d) ratio. In this

case, susceptibility (see Fig. 5b) with the increase in l:d demonstrates stronger dependence on the external field with the increase in the value of χ_z for small external fields and, otherwise, weaker dependence for large ones. However, because of the derease in the mean distance between chains, the possibility of the antiferromagnetic ordering of such chains increases that prevents further increase in the discrepancy of the dependeces $\langle u_z(h_z^{ext})\rangle$ and $\chi_z(h_z^{ext})$ with the increase in l:d.

Due to the fact that it is energetically favorable for nanoparticles to form chains exactly along the largest linear size, anisotropy of its magnetic properties will be observed. If external field is applied along the chain, then because of the codirectional dipole field ordering of the magnetic moments occurs rather intensively, and fast increase in the magnetization curve $\langle u_z(h_z^{ext})\rangle$ confirms this (Fig. 6a). At the same time, response along the orthogonal direction is considerably lower that is expressed in both flatter magnetization curve $\langle u_y(h_y^{ext})\rangle$ and weaker dependence of the susceptibility on the external field (see Fig. 6b).

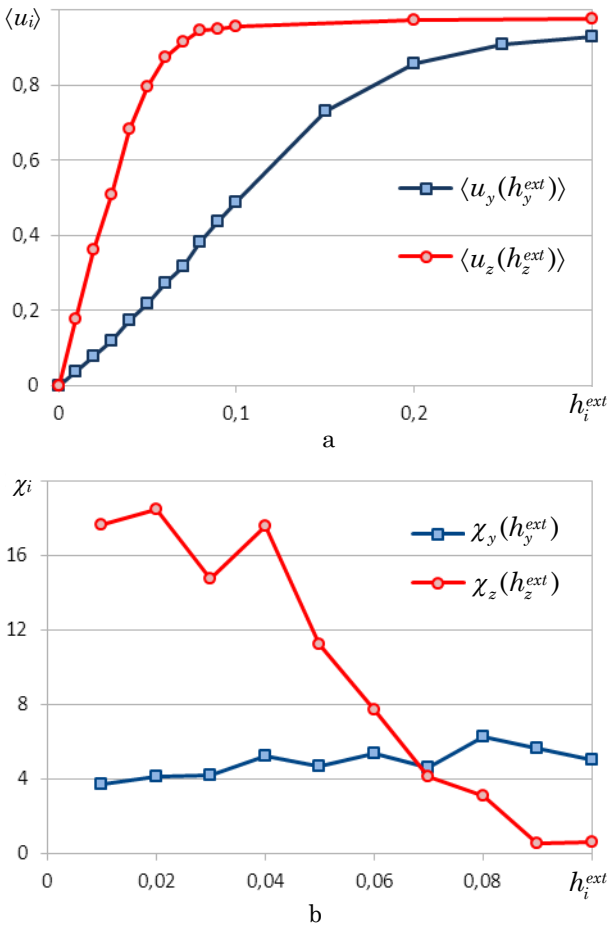

Fig. 6 – Anisotropy of the ferroliquid properties in elongated vessel: magnetization (a) and susceptibility (b) of ferrofluid. l:d = 1:5, ϕ = 5%

Another appearance of the anisotropy of properties consists in the noncoincidence of magnetization projections on the mutually perpendicular coordinate axes under the action along them of the same constant fields. If apply some external field ($h_y^{ext} = 0,3$ in Fig. 7) along the shorter vessel side and gradually change field h_z^{ext} along the longer side, then magnetization projection $\langle u_z\rangle$ will increase with larger velocity than projection $\langle u_y\rangle$ will drop (Fig. 7b). As a result, when both field projections will be equal ($h_y^{ext} = h_z^{ext} = 0,3$), condition $\langle u_y\rangle < \langle u_z\rangle$ will hold.

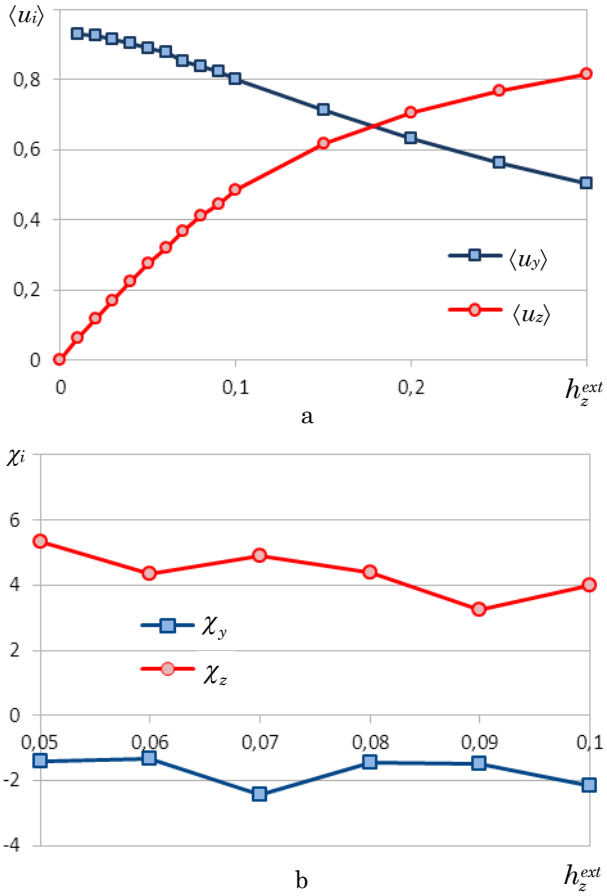

Fig 7 – Anisotropy of the magnetic properties at mutually perpendicular interaction of external fields: magnetization (a) and susceptibility (b) of ferrofluid. l:d = 1:5, ϕ = 5%

5. CONCLUSIONS

In the given work we present the simulation results of ferromagnetic liquid by the molecular dynamics method. In order to increase the speed, computing was carried out using GPU, and software implementation was performed by means of the CUDA technique. The key feature of the numerical simulation was application of the Barnes-Hut algorithm for the calculations of the interparticle interaction that allowed to simulate dynamics of the ensemble of 10^4 particles by using usual personal computer with low-cost video adapter.

The main aim of the investigations was establishment of the influence of interparticle interaction on the equilibrium properties of ferroliquid. It was shown that in the given question the key role belongs to the liquid structure which, in turn, is formed because of the dipole interaction. It is established that the process of cluster-

ing resulting either structure of the studied medium, depends on the number of factors, such as the volume content of particles, characteristics of additional repulsive forces provided due to the coating of nanoparticles by surfactants, temperature, and vessel form-factor.

At not very large volume fraction of particles, they form chains and dipole field amplifies the external one that leads to the increase in the susceptibility in comparison with the case of the interaction absence. With further increase in the particle fraction due to the possibility of the formation of the ring-shaped clusters or antiferromagnetic ordering of neighboring chains, the tendency to the decrease in the response of the medium to the external field begins to prevail and dependence of the susceptibility on the external field is weakened. The described tendencies can be significantly amplified if put ensemble into narrow vessel that indicates the anisotropy conditioned by the vessel form-factor that is not observed in the case when interaction is small.

If system magnetization does not achieve saturation, susceptibility demonstrates growth with temperature, since thermal fluctuations prevent clustering which decreases the ensemble response to the external field. If magnetization is close to the saturated one, susceptibility, otherwise, decreases due to thermal fluctuations.

Increase in the repulsive force between particles increases the mean distance between them that, in turn, attenuates the influence of correlations of the magnetic moment directions and complicates the formation of stable clusters. Therefore, with the increase in the parameter σ, slope of the dependence of the susceptibility on the external field increases with rather large its values at small external fields and fast asymptotic approximation to zero at the magnetization saturation.

AKNOWLEDGEMENTS

The given work has been performed under the partial financial support of the Ministry of Education and Science, Youth and Sport of Ukraine (state registration number 0112U001383).

REFERENCES

1. R. Rosensweig, *Ferrohydrodynamics* (Cambridge University Press: 1985).
2. B.J. Kim, Yu. Piao, N. Lee, Y.Il Park, In-H. Lee, J.-Ho Lee, S.R. Paik, T. Hyeon, *Adv. Mater.* **22**, 57 (2010).
3. Q.A. Pankhurst, J. Connolly, S.K. Jones, J. Dobson, *J. Phys. D: Appl. Phys.* **36**, R167 (2003).
4. A. Jordan, R. Scholz, P. Wust, H. Fahling, R. Felix, *J. Magn. Magn. Mater.* **201**, 413 (1999).
5. Ch. Kittel, *Introduction to Solid State Physics,* 8th ed. (Willey: 2005).
6. K.I. Morozov, A.V. Lebedev, *J. Magn. Magn. Mater.* **85**, 51 (1990).
7. Y.A. Buyevich, A.O. Ivanov, *Physica A* **190**, 276 (1992).
8. A.O. Ivanov, O.B. Kuznetsova, *J. Magn. Magn. Mater.* **252**, 135 (2002).
9. H. Gould, J. Tobochnik, *Computer Simulation Methods. Applications to Physical Systems* (Addison-Wesley Publishing: 1988).
10. R.W. Chantrell, A. Bradbury, J. Popplewell, S.W. Charles, *J. Phys. D: Appl Phys.* **13**, L119 (1980).
11. R.W. Chantrell, A. Bradbury, S.W. Charles, S. Menear, J. Popplewell, *J. Magn. Magn. Matter.* **31-34**, 958 (1983).
12. N.L. Tran, H.H. Tran, *J. Non-Cryst. Solid.* **357**, 996 (2011).
13. S.W. Davis, W. McCausland, H.C. McGahagan, C.T. Tanaka, M. Widom, *Phys. Rev. E* **59**, 2424 (1999).
14. G. Meriguet, M. Jardat, P. Turq, *J. Chem. Phys.* **121**, 6078 (2004).
15. Z. Wang, C. Holm, H.W. Muller, *Phys. Rev. E* **66**, 021405 (2002).
16. M. Shliomis, *Sov. Phys. Usp.* **17**, 153 (1974).
17. Yu.L. Klimontovich, *Sov. Phys. Usp.* **30**, 154 (1987).
18. L. Landau, E. Lifshitz, *Phys. Z. Sowjetunion* **8**, 153 (1935).
19. http://www.nvidia.ru/object/tesla-server-gpus-ru.html.
20. J. Sanders, E. Kandrot, *CUDA by Examples* (Addison-Wesley: 2011).
21. http://top500.org/list/2012/06/100/.
22. J. Barnes, P. Hut, *Nature* **324**, 446 (1986).
23. L. Greengard, V. Rokhlin, *J. Comput. Phys.* **73**, 325 (1987).
24. A.Yu. Polyakov, T.V. Lyutyy, S. Denisov, V.V. Reva, P. Hanggi, arXiv:1212.2934v1 (2012).